

This discussion paper is/has been under review for the journal The Cryosphere (TC).  
Please refer to the corresponding final paper in TC if available.

# Initial sea-ice growth in open water: properties of grease ice and nilas

A. K. Naumann<sup>1</sup>, D. Notz<sup>1</sup>, L. Håvik<sup>2</sup>, and A. Sirevaag<sup>2</sup>

<sup>1</sup>Max Planck Institute for Meteorology, Hamburg, Germany

<sup>2</sup>Bjerknes Centre for Climate Research, University of Bergen, Bergen, Norway

Received: 23 December 2011 – Accepted: 3 January 2012 – Published: 13 January 2012

Correspondence to: A. K. Naumann (ann-kristin.naumann@zmaw.de)

Published by Copernicus Publications on behalf of the European Geosciences Union.

TCD

6, 125–158, 2012

## Initial sea-ice growth in open water

A. K. Naumann et al.

Title Page

Abstract

Introduction

Conclusions

References

Tables

Figures

◀

▶

◀

▶

Back

Close

Full Screen / Esc

Printer-friendly Version

Interactive Discussion



## Abstract

To investigate initial sea-ice growth in open water, we carried out an ice-tank study with three different setups: grease ice grew in experiments with waves and in experiments with a current and wind, while nilas formed in a quiescent experimental setup. In this paper we focus on the differences in bulk salinity, solid fraction and thickness between these two ice types.

We find that the bulk salinity of the grease-ice layer remains almost constant until the ice starts to consolidate. In contrast, the bulk salinity of nilas is in the first hours of ice formation well described by a linear decrease of  $2.1 \text{ g kg}^{-1} \text{ h}^{-1}$  independent of air temperature. Such rapid decrease in bulk salinity can be understood qualitatively in the light of a Rayleigh number, the maximum of which is reached while the nilas is still less than 1 cm thick.

Comparing three different methods to measure solid fraction in grease ice based on (a) salt conservation, (b) mass conservation and (c) energy conservation, we find that the method based on salt conservation does not give reliable results if the salinity of the interstitial water is approximated as being equal to the salinity of the upper water layer. Instead the increase in salinity of the interstitial water during grease-ice formation must be taken into account. We find that the solid fraction of grease ice is relatively constant with values of 0.25, whereas it increases to values as high as 0.5 as soon as the grease ice consolidates at its surface. In contrast, the solid fraction of nilas increases continuously in the first hours of ice formation.

The ice thickness is found to be twice as large in the first 24 h of ice formation in the setup with a current and wind compared to the other two setups, since the wind keeps parts of the water surface ice free. The development of the ice thickness can be reproduced well with simple, one dimensional models given only the air temperature or the ice surface temperature.

TCD

6, 125–158, 2012

## Initial sea-ice growth in open water

A. K. Naumann et al.

Title Page

Abstract

Introduction

Conclusions

References

Tables

Figures

◀

▶

◀

▶

Back

Close

Full Screen / Esc

Printer-friendly Version

Interactive Discussion



## 1 Introduction

Sea-ice growth in turbulent water differs from sea-ice growth in quiescent water. In turbulent water, ice crystals accumulate at the surface, forming a grease-ice layer composed of individual ice crystals and small irregular clumps of ice crystals. In quiescent conditions, nilas, a thin elastic crust, forms at the surface, which is getting thicker when water molecules freeze to the ice–water interface. To gain a better understanding of the differences in initial sea-ice formation in turbulent and quiescent water, we conducted an ice-tank study focusing on the evolution of young sea ice.

Sea-ice growth in quiescent conditions has been analysed for a long time and sea-ice thickness evolution has successfully been modeled by Stefan (1889), Lebedev (1938, after Maykut, 1986), Anderson (1961) and Maykut (1986) among others. Sea-ice growth under turbulent conditions has been investigated far less often. Most related work was based on ice-tank studies, mainly using a wave setup only and focusing on a certain stage of sea-ice evolution. Martin and Kaufmann (1981) and Newyear and Martin (1997) showed that in grease ice the wave amplitudes are damped exponentially, while the solid fraction of the grease-ice layer increases with distance to the wave generator. They also found that grease ice consolidates at a critical solid fraction. Studies with a multidisciplinary focus have been described by Haas et al. (1999) and Wilkinson et al. (2009). Analysis of the latter study by de la Rosa et al. (2011) and de la Rosa and Maus (2011) gave results similar to that of Martin and Kaufmann (1981), namely that a critical solid fraction exists at which grease ice transforms to pancake ice. Dai et al. (2004) and Shen et al. (2004) focused on pancake ice and found that pancake ice thickness is influenced by rafting processes and that the pancake diameter is determined by the amplitude of the waves.

In contrast to the studies mentioned above, we conducted several experiments of ice formation in a tank in which both a quiescent and two different turbulent setups were realised. We were therefore able to directly investigate differences and similarities of sea-ice formation in quiescent and turbulent water. Additionally, the air temperature

TCD

6, 125–158, 2012

### Initial sea-ice growth in open water

A. K. Naumann et al.

Title Page

Abstract

Introduction

Conclusions

References

Tables

Figures

◀

▶

◀

▶

Back

Close

Full Screen / Esc

Printer-friendly Version

Interactive Discussion



was changed systematically to examine its influence on the properties of the forming sea ice. Analysing the properties of sea ice, we focus on its bulk salinity, solid fraction and thickness. To determine the solid fraction most studies use a method which is based on salinity measurements, although it is still not clear how reliable this method is.

5 We therefore test and compare three methods independent of each other to determine the solid fraction of a grease-ice layer.

Note that after finishing this manuscript, we became aware of a submitted paper by Maus and de la Rosa (J.Glac.) that addresses some of the topics that we discuss here. Note also that more details on our experiments and analysis can be found in Naumann (2011).

10 This paper is structured as follows: in Sect. 2 we describe the experimental setup of the tank and the three methods used to determine the solid fraction of the grease-ice layer. In Sect. 3 we give an overview of both the visible evolution of the ice layer and the measured development of the temperature and the salinity of the water under the ice during the experiments. In Sect. 4 we first analyse the three methods used to measure solid fraction in grease ice. Then we describe and discuss the bulk salinity and the solid fraction of grease ice and of nilas separately and in the end compare the properties of these two ice types with each other. In Sect. 5 we finally give some concluding remarks.

## 20 **2 Experimental setup**

### **2.1 Tank setup**

The experiments were conducted in a tank with a floor area of 194 cm × 66 cm, which was filled to 90 cm with NaCl solution. The tank was placed in a cold room and in total 17 experiments were conducted at fixed air temperatures between −5 °C and −20 °C. Each experiment lasted for 5 h to 48 h. The initial salinity of the water was about 29 g kg<sup>−1</sup>, but due to experimental processing it varied between 28 g kg<sup>−1</sup> and 30 g kg<sup>−1</sup>.

## Initial sea-ice growth in open water

A. K. Naumann et al.

Title Page

Abstract

Introduction

Conclusions

References

Tables

Figures

◀

▶

◀

▶

Back

Close

Full Screen / Esc

Printer-friendly Version

Interactive Discussion



## Initial sea-ice growth in open water

A. K. Naumann et al.

Title Page

Abstract

Introduction

Conclusions

References

Tables

Figures

◀

▶

◀

▶

Back

Close

Full Screen / Esc

Printer-friendly Version

Interactive Discussion



To restrict heat loss primarily to the surface area of the tank, 5 cm thick styrodur plates were fixed to the bottom and side walls of the tank. Heating plates were mounted to the sides of the tank at the height of the water surface to prevent freezing of ice to the walls. Additionally, a heating wire was installed at the bottom of the tank to prevent ice formation at the instruments due to supercooling.

We carried out a number of experiments with three different setups: six quiescent experiments, four experiments with waves and seven experiments with a current. In the quiescent experiments no movement was induced to the water in the tank. For the experiments with waves two pumps were adjusted to the resonance frequency of the tank, generating a standing wave with an amplitude of about 5 cm. In the experiments with a current, a plate divided the tank in two basins at the bottom but allowed for an oblonged circular track at the uppermost 30 cm. To avoid freezing of the pump that pushed the water around the tank, the pump was not placed at the surface but beneath the expected ice layer, inducing a maximum water velocity at 16 cm depth. An additional wind system was installed in the air just above the water to induce a surface current.

The tank was equipped with 4 CTDs (Conductivity, Temperature and Depth; SBE 37-SM MicroCAT) that measured salinity and temperature of the water in different depths (see Table 1). Because the CTDs were calibrated to measure sea-water salinity, but were used to measure NaCl solution salinity, conversion calculations had to be made. By preparing NaCl solutions of known salinity, we found that the difference  $\Delta S$  of sea-water salinity measured by the CTD  $S_{\text{CTD}}$  and the true NaCl solution salinity  $S_{\text{NaCl}}$  is a function of the temperature  $T_w$  and the salinity of the water, giving  $\Delta S = S_{\text{CTD}} - S_{\text{NaCl}} = 0.0517S_{\text{CTD}} - 0.0079T_w$ . In the temperature and salinity range used here this conversion corresponds to a subtraction of values between  $\Delta S = 1.2 \text{ g kg}^{-1}$  and  $\Delta S = 1.8 \text{ g kg}^{-1}$  from the sea-water salinity values measured with the CTDs (for details see Naumann, 2011).

Thermistors gave a vertical temperature profile with a resolution of up to 0.5 cm in the ice layer, the air layer above the ice and the water layer below the ice. An

additional thermometer (Young Platinum Temperature Probe, Model 41342) recorded the air temperature in 12 cm height above the ice surface.

In addition, turbulent heat, salt and momentum fluxes were recorded in the under-ice boundary layer during ice formation. A description and the analysis of these fluxes can be found in Håvik et al. (2012).

For a more detailed description of the tank setup and its instrumentation, see Naumann (2011).

## 2.2 Methods of solid-fraction measurement

In the experiments with waves and with a current, samples of the grease-ice layer were taken to measure the solid fraction of the ice layer. The solid fraction,  $\phi$ , is defined as the ratio of the mass of pure ice in the ice layer,  $m_i$ , to the total mass of the ice layer,  $m_t$ :

$$\phi = \frac{m_i}{m_t} \quad (1)$$

To determine the solid fraction of the ice layer, we used three methods, where the first is relying on conservation of salt, the second on conservation of mass and the third on conservation of energy.

The most commonly used method to measure the solid fraction in a grease-ice layer in the field or in a laboratory is based on conservation of salt (e.g., Smedsrud, 2001), in the following referred to as the salinity method. For the sample, salt and mass are conserved during melting. Mass conservation gives  $m_t = m_i + m_w$ , where  $m_w$  is the mass of the interstitial water in the ice layer. Salt conservation gives  $m_t S_t = m_i S_i + m_w S_w$ , where  $S_t$  is the salinity of the melted sample,  $S_w$  is the salinity of the interstitial water and  $S_i = 0 \text{ g kg}^{-1}$  is the salinity of the pure ice. For the solid fraction this leads to

$$\phi = \frac{S_w - S_t}{S_w}. \quad (2)$$

## Initial sea-ice growth in open water

A. K. Naumann et al.

Title Page

Abstract

Introduction

Conclusions

References

Tables

Figures

◀

▶

◀

▶

Back

Close

Full Screen / Esc

Printer-friendly Version

Interactive Discussion



## Initial sea-ice growth in open water

A. K. Naumann et al.

Title Page

Abstract

Introduction

Conclusions

References

Tables

Figures

◀

▶

◀

▶

Back

Close

Full Screen / Esc

Printer-friendly Version

Interactive Discussion



$S_t$  is measured directly in the melted sample (with a Hach HQ40d gauge), but an assumption has to be made for the salinity of the interstitial water,  $S_w$ . A commonly used assumption is that the salinity of the interstitial water between the ice crystals is equal to the salinity of the water under the ice layer (e.g., Smedsrud, 2001), which is here measured with the uppermost CTD. This assumption is, however, generally not justified because salt is rejected to the interstitial water when ice crystals are forming. The salinity of the interstitial water is therefore principally increased during ice formation. In the following, we introduce a second and a third method, which are independent of salinity, to estimate the accuracy of the salinity method.

The second method to determine the solid fraction is based on the volume difference of the sample before and after melting. We hence refer to it as the volume method. Mass conservation gives  $V_2\rho_{w,2} = V_1\rho_i\phi + V_1\rho_{w,1}(1 - \phi)$ , where  $V_1$  and  $V_2$  are the volume and  $\rho_{w,1}$  and  $\rho_{w,2}$  are the density of the sample before and after melting, respectively.  $\rho_i$  is the density of pure ice. For the solid fraction this leads to

$$\phi = \frac{\frac{V_2}{V_1}\rho_{w,2} - \rho_{w,1}}{\rho_i - \rho_{w,1}}. \quad (3)$$

For the third method the solid fraction of the ice layer is determined by relying on energy conservation and using a calorimeter. We therefore call this method calorimeter method. The heating wire of the calorimeter supplies an amount of heat  $\Delta Q$  to the sample that arises as the product of the potential  $U$ , the amperage  $I$  and the time  $\Delta t$  during which the wire is active. The supplied amount of heat melts the ice and warms the sample by the temperature difference  $\Delta T$ . Energy conservation gives  $\Delta Q = m_t c_p \Delta T + L m_t \phi$ , where  $c_p = 4010 \text{ J kg}^{-1} \text{ K}^{-1}$  is the specific heat capacity of salt water at  $T = 0^\circ \text{C}$  and  $S = 29.9 \text{ g kg}^{-1}$  (Bromley et al., 1967) and  $L = 332\,300 \text{ J kg}^{-1}$  is the heat of fusion for ice at  $T = -1.8^\circ \text{C}$  (Notz, 2005). For the solid fraction this leads to

$$\phi = \frac{UI\Delta t - m_t c_p \Delta T}{L m_t}. \quad (4)$$

The error due to measurement uncertainties (see Table 2) according to Gauß's error propagation law is  $\Delta\phi = 0.03$  for the salinity method and  $\Delta\phi = 0.02$  for the calorimeter method. For the volume method the error is as large as  $\Delta\phi = 0.24$  due to the small difference in volume of the sample before and after melting compared to the total volume of the sample.

### 2.3 Sampling method

To measure the solid fraction we took samples of the grease-ice layer every half an hour during the first hours of the experiments with waves and with a current. Since the different methods required different processing of the samples, not all three methods could be carried out on a single sample. Therefore each time two samples were taken where the first one was analysed with the calorimeter and the salinity method and the second one with the volume and the salinity method.

In the experiments with waves, the samples were taken in the middle of the tank. In the experiments with a current, the ice crystals first accumulated in the ends of the tank, which is why we shifted the region of sampling there. As a sampling device we used a pipe with a circular plate in the lower part that could be moved from a vertical position to a horizontal position with an attached stick (see Fig. 1). After lowering the pipe into the grease-ice layer, the pipe was sealed by moving the circular plate into a horizontal position with the stick. The pipe could then be lifted out of the tank and the sample was decanted in a graduated measuring glass or the bucket of a calorimeter to be processed further following the methods described in Sect. 2.2.

The samples taken from the grease-ice layer do not only consist of the grease-ice layer itself, but also always contain parts of the underlying water (Fig. 1). In order to obtain the solid fraction of the grease-ice layer (in contrast to the solid fraction of the whole sample), the solid fraction of the grease-ice layer was calculated with the three methods introduced in Sect. 2.2 and by additionally compensating for the ratio of the grease-ice layer to the water layer in the sample. If the grease-ice layer in the sample was thinner than 1.5 cm, the sample was not analysed, because the error

## Initial sea-ice growth in open water

A. K. Naumann et al.

Title Page

Abstract

Introduction

Conclusions

References

Tables

Figures

◀

▶

◀

▶

Back

Close

Full Screen / Esc

Printer-friendly Version

Interactive Discussion



then becomes very sensitive to grease-ice layer thickness measurements: a typical measurement inaccuracy of 0.5 cm corresponds to an over- or underestimation of 30 % of the solid fraction.

Note that in contrast to the well mixed water of the turbulent experiments, the upper water layer was stratified in temperature during the quiescent experiments (see Sect. 3). Sample taking in the forming ice layer of the quiescent experiments would disturb this layering. Also, it was not possible for us to take samples from nilas without draining off of brine because the thin ice was still very porous. Hence sample taking was not performed during the quiescent experiments. Instead, the solid fraction was estimated from the bulk salinity and the temperature of the ice layer (see Sect. 4.3).

### 3 General observations

Having described the experimental setup and the methods used to determine the solid fraction, we now describe the visible evolution of the ice layer and the measured development of the temperature and the salinity of the water under the ice for the different setups.

The visible evolution of the ice layer differed substantially between the different setups but not between the various experiments of one setup. In the quiescent experiments a closed, solid ice cover of nilas formed as soon as the experiment started. Spatially the ice layer was uniformly thick and covered the whole surface area of the tank. For the experiments with waves, first a pure grease-ice layer appeared, before pancake ice with an ice crystal layer in between formed. Apart from the small fraction of surface area directly influenced by the water filling and leaving the pumps, the ice layer covered the whole surface with a roughly spatially uniform thickness as in the quiescent setup. In the experiments with a current the water circulated clockwise in the tank carrying small ice discs with a diameter of a few millimeters in the first five to ten minutes of ice formation. Thereafter, ice crystals appeared and accumulated at the ends of the tank, where they formed a grease-ice layer that was considerably thicker

## Initial sea-ice growth in open water

A. K. Naumann et al.

Title Page

Abstract

Introduction

Conclusions

References

Tables

Figures

◀

▶

◀

▶

Back

Close

Full Screen / Esc

Printer-friendly Version

Interactive Discussion



than in the quiescent experiments or the experiments with waves. At the same time, the straight parts of the track stayed ice free at least for the first approximately four hours, mainly due to the installed wind. Later the grease-ice layer started to consolidate at the surface and the ice edge slowly advanced into the straight parts of the track. Our setup with a current is hence more representative for a wind-driven situation like a polynya than for a situation with a current only. However, for consistency we stick to the term “experiment with a current” in the following.

Figure 2 shows the development of water temperature and salinity for one of the experiments with a current. Temperature and salinity are the vertical averages over the values obtained from the four CTDs (see Table 1). The water temperature decreased in the first one and a half hours until the freezing point of the water was reached. At this point the salinity of the water started to increase due to the beginning of ice formation. Within 24 h the salinity of the water increased by about  $1 \text{ g kg}^{-1}$ , which is equivalent to a gain of  $30 \text{ kg m}^{-2}$  pure ice.

In the experiments with a current and with waves, the development of water temperature and salinity was similar. For the quiescent experiments, the fluctuations in water temperature and salinity were more pronounced (not shown) because of the absence of pump-induced mixing. In these experiments, the water temperature as measured by all four CTDs was some tenth of a degree higher than the freezing point, up to  $-1.5^\circ\text{C}$ . This indicates a very strong stratification towards the ice–water interface in the quiescent experiments.

## 4 Results

After focusing on the visible evolution of the ice layer and the measured development of the temperature and the salinity of the water during the experiments, we now analyse the three methods used to measure solid fraction in grease ice in Sect. 4.1. Then we describe and discuss the measured properties of the ice layer separately for grease ice and nilas in Sects. 4.2 and 4.3, respectively. In Sect. 4.4 we finally compare the properties of grease ice and nilas.

### Initial sea-ice growth in open water

A. K. Naumann et al.

Title Page

Abstract

Introduction

Conclusions

References

Tables

Figures

◀

▶

◀

▶

Back

Close

Full Screen / Esc

Printer-friendly Version

Interactive Discussion



## 4.1 Methods of solid-fraction measurements

As outlined in the introduction, it is not clear how reliable the different methods used to measure the solid fraction of an ice layer are. We therefore used three different methods to determine the solid fraction in the grease-ice layer (Sect. 2.2). Solid fractions estimated with the salinity method from different samples, but at the same time, compare very well (Fig. 3), indicating no large differences between two samples taken at the same time at slightly different places.

While the solid fraction values from the calorimeter and the volume method agreed very well with each other, the values of the solid fraction obtained from the salinity method underestimated the values of the solid fraction measured with the calorimeter or the volume method by about 50% (Fig. 3). This underestimation is likely due to the assumption made for the salinity method that the salinity of the interstitial water is equal to the salinity of the water under the ice. When ice is forming from salt water, salt molecules can not be incorporated into the ice-crystal structure, but will be rejected to the surrounding water. With a decreasing temperature of the grease-ice layer, the salinity of the interstitial water is increasing to maintain phase equilibrium. By fitting the data of Weast (1971), a relationship between the temperature and the salinity of a NaCl solution in phase equilibrium can be described by

$$S = -0.35471 - 17.508T - 0.33518T^2 \quad (5)$$

with a maximum error of  $\Delta S = 0.005 \text{ g kg}^{-1}$  or  $\Delta T = 0.001 \text{ }^\circ\text{C}$  in the considered range of salinities from  $S = 20 \text{ g kg}^{-1}$  to  $S = 40 \text{ g kg}^{-1}$  or water temperatures from  $T = -1.2 \text{ }^\circ\text{C}$  to  $T = -2.4 \text{ }^\circ\text{C}$ . We find vertical mean grease-ice temperatures from  $T = -1.8 \text{ }^\circ\text{C}$  to  $T = -2.3 \text{ }^\circ\text{C}$  which corresponds to salinities of the interstitial water between  $S = 30.1 \text{ g kg}^{-1}$  and  $S = 38.1 \text{ g kg}^{-1}$  (Eq. 5). Unfortunately, the grease-ice temperature could not be determined more accurately in our setup because the ice surrounding the thermistor string was not representative for grease ice. However, modifying the assumption of the salinity method such that the salinity of the interstitial water is now assumed to be  $35 \text{ g kg}^{-1}$  instead of equal to the salinity of the water under the ice ( $29 \text{ g kg}^{-1}$ ),

### Initial sea-ice growth in open water

A. K. Naumann et al.

Title Page

Abstract

Introduction

Conclusions

References

Tables

Figures

◀

▶

◀

▶

Back

Close

Full Screen / Esc

Printer-friendly Version

Interactive Discussion



leads to a mean solid fraction calculated with the salinity method that is increased to  $\phi = 0.25$ . This is in good agreement with the calorimeter and the volume method. In a field setup, we suggest to measure the grease-ice surface temperature (e.g. with an IR-thermometer) and assume a linear temperature profile to the grease-ice–water interface to be able to calculate the salinity of the interstitial water with Eq. (5).

Figure 4 shows the distribution of the calculated solid fraction for the calorimeter method and the volume method. The values of the volume method show a wider distribution than the values of the calorimeter method due to the larger error of the volume method.

## 4.2 Properties of grease ice

Comparing the results of the three methods discussed above, it is striking that the mean of the solid fraction of the grease-ice layer is not showing a clear trend over time, with values of about  $\phi = 0.25$  for the volume and the calorimeter method (Fig. 3). The same result holds for the individual experiments. Furthermore we do not see a dependence of the solid fraction on the air temperature (not shown). For the calorimeter method 90 % of the values are between  $\phi = 0.07$  and  $\phi = 0.38$  and 50 % are between  $\phi = 0.15$  and  $\phi = 0.28$  (Fig. 4a). In contrast, the mean of the solid fraction of newly consolidated ice in the turbulent experiments is  $\phi_{\text{cons.}} = 0.35$  for the experiments with a current and  $\phi_{\text{cons.}} = 0.5$  for the experiments with waves (not shown). The differences in solid fraction of newly consolidated ice in the experiments with a current and with waves arise since even after the consolidation of the ice layer at its surface, a grease ice layer exists in the lower parts of the ice layer. As this grease-ice layer under the consolidated ice layer is thicker in the experiments with a current (Sect. 3), the vertical mean solid fraction of the newly consolidated ice layer in the experiments with a current is lower than in the experiments with waves.

A possible reason for the constant solid fraction of the grease ice before its consolidation is the geometrical packing of the ice crystals in the grease-ice layer. Imagining the forming grease-ice layer as randomly orientated ice crystals rising to the surface due to

## Initial sea-ice growth in open water

A. K. Naumann et al.

Title Page

Abstract

Introduction

Conclusions

References

Tables

Figures

◀

▶

◀

▶

Back

Close

Full Screen / Esc

Printer-friendly Version

Interactive Discussion



buoyancy, they only occupy a certain part of the volume of the forming grease-ice layer. The emergence of new ice crystals increases the volume of the grease-ice layer but not its solid fraction, leading to a constant solid fraction over time in the grease-ice layer as observed. Only the consolidation of a grease-ice layer on its surface then leads to an increasing solid fraction, which we also observed.

To get an estimate of the solid fraction of an ice-crystal layer with such randomly orientated ice crystals, we assume for simplicity that the ice crystals are discs with a certain diameter to height ratio  $H$ . A disc is put into a cuboid so that it is in contact with the wall. If the disc is lying in parallel to the cuboids base area the disc takes 78.5 % of the cuboids volume. If the crystal is inclined to form an angle  $\alpha$  to the cuboids base area (Fig. 5) the solid fraction is given as

$$\phi = \frac{\rho_i}{\rho_w} \frac{\pi}{4H \left( \frac{\sin \alpha}{H} + \cos \alpha \right) \left( \frac{\cos \alpha}{H} + \sin \alpha \right)}, \quad (6)$$

where the factor  $\frac{\rho_i}{\rho_w}$  accounts for the conversion to a mass solid fraction instead of a volume solid fraction. In a wall to wall packing of cuboids, the discs would not necessarily touch each other so that this estimate should be seen as a lower boundary estimate. With a diameter to height ratio of  $H = 10$  (as used in Omstedt, 1985) and randomly orientated discs (average of  $\alpha = 0^\circ$  to  $\alpha = 89^\circ$ ) Eq. (6) gives  $\phi = 0.22$ , which is only slightly less than the measured solid fraction and therefore fits our data very well. However, it should be noted that other values for the diameter to height ratio found in literature are in part up to a magnitude higher than the value used here (e.g., Martin and Kaufmann, 1981; Weeks and Ackley, 1986), which would lead according to Eq. (6) to estimated solid fractions that are considerably lower than  $\phi = 0.22$ .

Another explanation for the rather constant solid fraction can directly be obtained from the so-called mushy-layer equations (see, for example, Hunke et al., 2011). These equations describe the evolution of general multi-phase, multi-component systems, like sea ice. As long as the Rayleigh number (see Sect. 4.3) is sufficiently small to hinder convective overturning and loss of the salty brine between the ice crystals, and as long

**Initial sea-ice growth  
in open water**

A. K. Naumann et al.

Title Page

Abstract

Introduction

Conclusions

References

Tables

Figures

◀

▶

◀

▶

Back

Close

Full Screen / Esc

Printer-friendly Version

Interactive Discussion



## Initial sea-ice growth in open water

A. K. Naumann et al.

Title Page

Abstract

Introduction

Conclusions

References

Tables

Figures

◀

▶

◀

▶

Back

Close

Full Screen / Esc

Printer-friendly Version

Interactive Discussion



as the surface temperature is constant, the mushy-layer equations admit a similarity solution for the solid-fraction distribution within sea ice (e.g., Chiareli and Worster, 1992). Our measurements show an almost constant bulk salinity (Fig. 6) and only very small changes of the surface temperature during the first few hours of the experiment. Independent of geometrical packing, the similarity solution of the mushy layer equations predict a constant mean solid fraction, with higher solid fraction towards the surface and lower solid fraction towards the ice–ocean interface.

Unfortunately, the vertical resolution of our sampling is too low to allow us to ultimately pin down the constant solid fraction to the geometry argument (which predicts a rather uniform vertical solid-fraction profile) or the similarity solution argument (which predicts a vertically varying solid-fraction profile).

The bulk salinity,  $S_{bu}$ , of the grease-ice layer can be determined from the measured salinity of the melted sample, the (volume) ratio of the grease-ice layer to the whole sample and the salinity of the water under the ice layer measured by the uppermost CTD. Values of the calculated bulk salinity of the grease-ice layer vary between  $S_{bu} = 24 \text{ g kg}^{-1}$  and  $S_{bu} = 29 \text{ g kg}^{-1}$ , are independent of air temperature and almost constant in time (Fig. 6). The mean value of the bulk salinity  $S_{bu} = 26.5 \text{ g kg}^{-1}$  is about  $3 \text{ g kg}^{-1}$  less than the initial salinity of the water under the ice.

### 4.3 Properties of nilas

There is very little published data available on the salinity evolution of very thin ice. Most data sets (for example Cox and Weeks, 1974) only report on the salinity of sea ice with a thickness of more than 10 cm, which is the minimum thickness to safely work on sea ice in field conditions. In our lab experiments, however, we are able to calculate the bulk salinity,  $S_{bu}$ , of the ice layer from the onset of its formation by applying salt conservation in the tank and considering the measured change in salinity of the water underneath the ice as well as the ice thickness. Figure 7a shows the evolution of the bulk salinity in the different quiescent experiments with time and a least square fit to the data.

The bulk salinity decreases in all the quiescent experiments, i.e. independent of air temperature, in the first seven to ten hours from values of  $29 \text{ g kg}^{-1}$  to about  $10 \text{ g kg}^{-1}$ . After ten hours the bulk salinity barely decreases and stays relatively constant. The linear least square fit of all values measured in the first ten hours of each experiment gives a decrease of  $2.1 \text{ g kg}^{-1} \text{ h}^{-1}$ . We are currently carrying out a detailed modeling study to further investigate the underlying reasons for the rather linear decrease in bulk salinity independent of air temperature in very thin ice.

The rapid decrease of bulk salinity in the first hours of ice formation can be understood by considering the Rayleigh number,  $Ra$ . The Rayleigh number is defined as the ratio of available potential energy due to density differences between the brine and the underlying water and the dissipative impact of diffusion and viscosity,

$$Ra = \frac{g(\rho_w - \rho_{br})\Pi h}{\mu\kappa}, \quad (7)$$

where  $g$  is gravity,  $\mu$  the dynamic viscosity of the brine and  $\kappa$  the thermal diffusivity of the brine.  $\Pi$  is the permeability of the ice layer, which can be approximated as a function of the solid volume fraction,  $\phi_v$ , by the empirical relationship  $\Pi = 10^{-17}(10^3(1 - \phi_v))^{3.1} \text{ m}^2$  as formulated by Freitag (1999). Because the brine temperature determines the salinity of the brine, the density of the brine near the ice surface  $\rho_{br}$  depends only on the brine temperature, which was measured with the thermistors.

When the Rayleigh number exceeds a critical value of about  $Ra=10$  (e.g., Worster, 1992; Wettlaufer et al., 1997; Notz and Worster, 2008) convection of brine starts. The bulk salinity then decreases due to gravity drainage, which is the only process that leads to considerable salt loss in sea ice during freezing (Notz and Worster, 2009; Wells et al., 2011). In this study, the maximum of the Rayleigh number at the ice surface was reached in all experiments within the first 2.5 h after the onset of freezing (Fig. 7b) which corresponds to an ice thickness of less than 1 cm. Therefore the early and fast decrease in bulk salinity is in good agreement with the evolution of the Rayleigh number. We do not see a delay in salt release from Nilas as measured by Wettlaufer

## Initial sea-ice growth in open water

A. K. Naumann et al.

Title Page

Abstract

Introduction

Conclusions

References

Tables

Figures

◀

▶

◀

▶

Back

Close

Full Screen / Esc

Printer-friendly Version

Interactive Discussion



et al. (1997) in a tank experiment with a cooling plate in direct contact with the water surface. This difference is caused by the fact that in our experiments the surface temperature of the ice evolves freely, causing the initial ice to be relatively warm and hence more permeable than the thin ice in the Wettlaufer et al. (1997) experiments.

Knowing the bulk salinity and the ice temperature, the solid fraction of the ice layer can be calculated. For the bulk salinity one has  $S_{bu} = S_i\phi + S_{br}(1 - \phi)$ , which gives with  $S_i = 0 \text{ g kg}^{-1}$

$$\phi = 1 - \frac{S_{bu}}{S_{br}}. \quad (8)$$

The brine salinity  $S_{br} = S_{br}(T_i)$  is a function of the ice temperature  $T_i$  (see Eq. 5) which was measured by the thermistors. For calculating the bulk salinity the fits shown in Fig. 7a were used.

The solid fraction increases fast in the first seven hours after the onset of freezing to values of  $\phi = 0.7$  to  $\phi = 0.8$ , where low solid fraction corresponds to high air temperature and vice versa (Fig. 7c). The increase in solid fraction is due to the decreasing bulk salinity (because salty brine is draining off the ice layer) and an increasing brine salinity (ice temperature is decreasing). After seven hours the solid fraction stays almost constant and increases only slightly. The local minima in the solid fraction every sixths hour in Fig. 7c are caused by air temperature variations due to defrosting periods of the cooling system. The periods are clearly seen in the ice temperature and in this way influence the solid fraction of the ice layer.

#### 4.4 Comparison of properties of grease ice and nilas

After discussing the bulk salinity and the solid fraction development with time in the first hours of ice formation for grease ice and nilas separately (Sects. 4.2 and 4.3), these two can now be compared.

In Fig. 8a the averages of the bulk salinity over all experiments with waves and with a current are shown as well as the fit to the data in the quiescent experiments. Bulk

## Initial sea-ice growth in open water

A. K. Naumann et al.

Title Page

Abstract

Introduction

Conclusions

References

Tables

Figures

◀

▶

◀

▶

Back

Close

Full Screen / Esc

Printer-friendly Version

Interactive Discussion



salinities are normalised with the initial salinity of the water at the beginning of the experiments (compare to Figs. 6 and Fig. 7a). The average normalised bulk salinity of the grease-ice layer measured in this study is 0.9 and therefore on average higher than the values measured by Smedsrud and Skogseth (2006) in a fjord in Svalbard. In 5 cm to 20 cm thick grease ice, they found an average bulk salinity of  $S_{bu} = 26.0$  psu while their average ocean salinity was 34.5 psu giving a normalised salinity of 0.75.

The bulk salinity of the solid ice layer in the quiescent experiments begins to decrease when convection in the brine channels of the ice layer starts. According to the Rayleigh number, convection starts at an ice thickness of less than 1 cm and is well described by a linear decrease of  $2.1 \text{ g kg}^{-1} \text{ h}^{-1}$  in the first seven hours of freezing. The often used fit to field data by Cox and Weeks (1974) could not map this early and fast decrease of bulk salinity as the data came from sea ice that had a thickness of at least 10 cm. However, Cox and Weeks (1974) extrapolated their fit to thinner ice giving a bulk salinity of about  $S_{bu} = 14 \text{ g kg}^{-1}$  at an ice thickness of 2 cm which is in good agreement with our data after the fast, initial decrease.

Closely linked to the bulk salinity, the solid fraction also developed differently with time in the quiescent experiments compared to the experiments with waves or with a current. In Fig. 8b the averages of the solid fraction over all experiments with the same general setup are shown. For the experiments with waves and with a current this mean was obtained as the average of the calorimeter and the volume method.

The solid fraction of an ice layer increases with decreasing ice temperature and decreasing bulk salinity. As the ice got thicker with time in the quiescent experiments, the vertically averaged ice temperature decreased as did the bulk salinity (Fig. 7a). Hence in the quiescent experiments the solid fraction is increased from  $\phi = 0.10$  to  $\phi = 0.55$  within 4.5 h (Fig. 8b). Contrary to the quiescent experiments, the solid fraction in the grease-ice layer stayed constant in the first 3.5 h with values of about  $\phi = 0.25$  for both the experiments with waves and the experiments with a current. This might be due to the geometrical packing of the ice crystals in the grease-ice layer or be understood in the light of the similarity solution of the mushy-layer equations (Sect. 4.2). An increased

**Initial sea-ice growth  
in open water**

A. K. Naumann et al.

Title Page

Abstract

Introduction

Conclusions

References

Tables

Figures

◀

▶

◀

▶

Back

Close

Full Screen / Esc

Printer-friendly Version

Interactive Discussion



solid fraction of up to  $\phi_{\text{cons.}} = 0.5$  was observed for the newly consolidated ice layer in the turbulent experiments (not shown), which is comparable to the solid fraction in the quiescent experiments after 5 h.

The observed values of the solid fraction of the grease-ice layer are in good agreement with other laboratory studies. Martin and Kaufmann (1981) measured, depending on the amplitude of their wave field, ice concentrations of up to 40 % by sieving their grease-ice samples. In their work they also mentioned that the sieved grease-ice samples consisted of 72 % fresh-water ice and 28 % brine, which translates their concentration to a solid fraction of  $\phi = 0.29$ . De la Rosa and Maus (2011) measure a solid volume fraction of grease ice in a wave field and state that grease ice starts to form a consolidated surface at a critical solid volume fraction of  $\phi_v = 0.3$ . Their critical value corresponds to a solid fraction of  $\phi = 0.27$  and is therefore also in good agreement with the observed mean solid fraction of  $\phi = 0.25$  in this study.

Despite this good agreement in critical solid fraction, Martin and Kaufmann (1981) and de la Rosa and Maus (2011) also measured a spatial and temporal development of solid fraction, respectively. They found solid fraction values as low as  $\phi = 0.1$  in forming grease ice, when the ice crystals were still kept in suspension by turbulence due to waves. As the wave amplitude in our wave experiments was only about 5 cm and the ice crystals accumulated in the ends of the tank to a motionless grease-ice layer in the experiments with a current, we measured ice layer properties in a grease-ice layer almost at rest. Within a few hours this grease-ice layer started to form a solid ice layer. Our measurements are therefore not comparable to the early stage measurements of de la Rosa and Maus (2011) or the measurements in the direct proximity to the wave generating paddle of Martin and Kaufmann (1981).

In addition to the bulk salinity and the solid fraction of the ice layer, the third parameter that describes the ice layer is the ice thickness. In the quiescent experiments the ice thickness was read directly from a ruler at the tank wall since the ice thickness was distributed spatially very homogeneous in the tank. In the experiments with a current and with waves, an average ice thickness had to be estimated indirectly because of

## Initial sea-ice growth in open water

A. K. Naumann et al.

Title Page

Abstract

Introduction

Conclusions

References

Tables

Figures

◀

▶

◀

▶

Back

Close

Full Screen / Esc

Printer-friendly Version

Interactive Discussion



## Initial sea-ice growth in open water

A. K. Naumann et al.

Title Page

Abstract

Introduction

Conclusions

References

Tables

Figures

◀

▶

◀

▶

Back

Close

Full Screen / Esc

Printer-friendly Version

Interactive Discussion



a spatially very inhomogeneous ice-layer thickness and a moving ice layer, respectively. Such an estimate of ice thickness can be obtained from the measured salinity increase in the tank and the known bulk salinity and solid fraction of the ice layer, since the salinity increase in the water is due to salt release from the forming ice. According to the results in Sect. 4.2 the solid fraction of the ice layer in the experiments with waves and with a current is assumed to be  $\phi = 0.25$  in the first two hours. From four hours onwards an ice layer with a consolidated surface dominates. Therefore the solid fraction is estimated to be  $\phi_{\text{cons.}} = 0.35$  in the experiments with a current and  $\phi_{\text{cons.}} = 0.5$  in the experiments with waves. Between two and four hours after the onset of freezing a linear increase in solid fraction is assumed.

The resulting ice thickness development is shown in Fig. 8c. While the ice thickness in the quiescent experiments increases about as fast as in the experiments with waves, the ice thickness grows about twice as fast in the experiments with a current. The heat flux from relatively warm water to cold air is higher for open water than when an isolating ice cover is present (Maykut, 1982). Due to the open water area that was preserved mainly by the wind in the experiments with a current but not in the quiescent experiments or the experiment with waves (Sect. 3), heat loss is more efficient in the experiments with a current, i.e. the ice grows faster.

The ice thickness development in the quiescent experiments and the experiments with a current can be reproduced well with simple, one dimensional models. For the quiescent ice growth, a linear temperature profile in the ice layer with a surface temperature  $T_0$  and a ice–water interface temperature at its freezing point  $T_f$  is assumed. For the heat flux through the ice this gives  $k(T_f - T_0)/h$  (Stefan, 1889), where  $h$  is the ice thickness. The thermal conductivity  $k$  is  $k_i = 2.2 \text{ W m}^{-1} \text{ K}^{-1}$  for pure ice and  $k_{\text{br}} = 0.5 \text{ W m}^{-1} \text{ K}^{-1}$  for brine, giving  $k = k_i\phi + k_{\text{br}}(1 - \phi)$  for sea ice. If all water was at its freezing point, the heat flux through the ice is equal to the heat that is released due

to ice growth,  $k(T_f - T_0)/h = \phi \rho_i L (dh)/(dt)$  (Stefan, 1889). Integration gives

$$h(t) = \sqrt{\frac{2}{\rho_i L} \int_0^t \frac{k(T_f - T_0)}{\phi} dt}, \quad (9)$$

where  $\phi$  is given according to Eq. (8).

For the grease-ice model a constant temperature independent of depth is assumed in the grease-ice layer and the underlying water. The heat flux at the ice–air interface is proportional to the difference of the water temperature  $T_w$  and the air temperature  $T_a$  (measured in 12 cm height above the ice surface) multiplied with the heat transfer coefficient  $C$ , that has been calculated from measurement in the quiescent experiments to be  $C = 20 \text{ W m}^{-2} \text{ K}^{-1}$  (Naumann, 2011). Again this heat flux is equal to the heat that is released when ice is forming, therefore  $C(T_w - T_a) = \phi \rho_i L (dh)/(dt)$  (Maykut, 1986). Integration gives

$$h(t) = \frac{C}{\rho_i L} \int_0^t \frac{T_w - T_a}{\phi} dt, \quad (10)$$

where  $\phi$  is estimated according to the results in Sect. 4.2.

With these two simple models the ice thickness evolution can be estimated from the ice surface temperature for the quiescent case or the air temperature for the grease-ice model. In Fig. 8c the modeled ice thickness is shown together with the measured ice thickness evolution. Indeed, the ice thickness from the grease-ice model compares well with the measured ice thickness in the experiment with a current. The grease-ice thickness is only modeled up to seven hours since the solid fraction is not known afterwards. Also the ice thickness from the model for quiescent ice growth compares well with the ice thickness in the quiescent experiment.

## Initial sea-ice growth in open water

A. K. Naumann et al.

Title Page

Abstract

Introduction

Conclusions

References

Tables

Figures

◀

▶

◀

▶

Back

Close

Full Screen / Esc

Printer-friendly Version

Interactive Discussion



## 5 Summary and conclusions

To gain a better understanding of initial sea-ice formation in quiescent and turbulent water, we conducted a tank study with three different setups. We are therefore able to directly compare differences and similarities of sea-ice formation in quiescent and turbulent water.

We presented new measurements of bulk salinity in very thin sea ice grown from quiescent water, finding that it is well described by a linear decrease in the first hours of ice formation independent of air temperature. In weakly turbulent water, we find the bulk salinity to stay almost constant as long as grease ice is present.

Measuring the solid fraction of a grease-ice layer, we find that it is constant in the first hours of ice formation with an average value of  $\phi = 0.25$ , which is in good agreement with geometrical considerations and the work of Martin and Kaufmann (1981) and de la Rosa and Maus (2011). From a modeler's perspective it hence seems sufficient to use a constant solid fraction as long as grease ice is present. When the ice layer begins to consolidate from the surface, the solid fraction starts to increase. In contrast to the grease-ice layer, the solid fraction of nilas increases continuously.

We confirm that the development of the ice thickness is primarily influenced by the open water area as the heat flux from the water to the air is larger here than in the presence of a closed ice cover (Maykut, 1982). In our study the ice thickness grew twice as fast in the experiments with a current as in the quiescent experiments or the experiments with waves, since in the experiments with a current an open-water area remained at the surface throughout much of the experiment. The evolution of the ice thickness in these experiments could be reproduced well with simple, one dimensional models.

Additionally, three different methods to calculate the solid fraction from sample measurements in a grease-ice layer were tested because it was not clear yet which methods give reliable results. For the salinity method to reveal values which are in agreement with the calorimeter or the volume method, the salinity of the interstitial

TCD

6, 125–158, 2012

### Initial sea-ice growth in open water

A. K. Naumann et al.

Title Page

Abstract

Introduction

Conclusions

References

Tables

Figures

◀

▶

◀

▶

Back

Close

Full Screen / Esc

Printer-friendly Version

Interactive Discussion



**Initial sea-ice growth  
in open water**

A. K. Naumann et al.

[Title Page](#)[Abstract](#)[Introduction](#)[Conclusions](#)[References](#)[Tables](#)[Figures](#)[I◀](#)[▶I](#)[◀](#)[▶](#)[Back](#)[Close](#)[Full Screen / Esc](#)[Printer-friendly Version](#)[Interactive Discussion](#)

water must not be approximated with the salinity of the upper water layer. Instead, the salinity increase of the interstitial water of the grease-ice layer must be taken into account. Because the grease-ice layer has to remain in phase equilibrium, the salinity of the interstitial water of the grease-ice layer is determined by the temperature of the grease-ice layer. Based on the challenge to determine an average grease-ice temperature for the salinity method and the comparatively large error of the volume method, we recommend to use the calorimeter method to measure the solid fraction of a grease-ice layer at least in the laboratory, where immediate sample processing and power supply is no difficulty. For field measurements, we suggest to determine the grease-ice surface temperature and assume a linear temperature profile to the grease-ice–water interface, to be able to obtain reliable results from the salinity method.

The service charges for this open access publication have been covered by the Max Planck Society.

*Acknowledgements.* We thank Iris Ehlert for helpful comments that improved this manuscript. We acknowledge financial support through a Max Planck Research Group, the German Academic Exchange Service (DAAD) and the Research Council of Norway.

## References

Anderson, D. L.: Growth rate of sea ice, *J. Glaciol.*, 3, 1170–1172, 1961.

Bromley, L. A., Desaussure, V. A., Clipp, J. C., and Wright, J. S.: Heat capacities of sea water solutions at salinities of 1 to 12 % and temperatures of 2 °C to 80 °C, *J. Chem. Eng. Data*, 12, 202–206, doi:10.1021/je60033a013, 1967. 131

Chiareli, A. O. P. and Worster, M. G.: On measurements and prediction of the solid fraction within mushy layers, *J. Cryst. Growth*, 125, 487–494, 1992. 138

Cox, G. F. N. and Weeks, W. F.: Salinity variations in sea ice, *J. Glaciol.*, 13, 109–120, 1974. 138, 141

Dai, M., Shen, H. H., Hopkins, M. A., and Ackley, S. F.: Wave rafting and the equilibrium

**Initial sea-ice growth  
in open water**

A. K. Naumann et al.

Title Page

Abstract

Introduction

Conclusions

References

Tables

Figures

◀

▶

◀

▶

Back

Close

Full Screen / Esc

Printer-friendly Version

Interactive Discussion



pancake ice cover thickness, *J. Geophys. Res.*, 109, C07023, doi:10.1029/2003JC002192, 2004. 127

De la Rosa, S. and Maus, S.: Laboratory study of frazil ice accumulation under wave conditions, *The Cryosphere Discuss.*, 5, 1835–1886, doi:10.5194/tcd-5-1835-2011, 2011. 127, 142, 145

De la Rosa, S., Maus, S., and Kern, S.: Thermodynamic investigation of an evolving grease to pancake ice field, *Ann. Glaciol.*, 52, 206–214, 2011. 127

Freitag, J.: Untersuchungen zur Hydrologie des arktischen Meereises – Konsequenzen für den kleinskaligen Stofftransport, *Berichte zur Polarforschung* 325, Alfred-Wegener Institut für Polar- und Meeresforschung, Bremerhaven, 1999 (in German). 139

Haas, C., Cottier, F., Smedsrud, L. H., Thomas, D., Buschmann, U., Dethleff, D., Gerland, S., Giannelli, V., Hoelemann, J., Tison, J.-L., and Wadhams, P.: Multidisciplinary ice tank study shedding new light on sea ice growth processes, *EOS T. Am. Geophys. Un.*, 80, 507, doi:10.1029/EO080i043p00507-01, 1999. 127

Håvik, L., Sirevaag, A., Naumann, A. K., and Notz, D.: Growing ice in a tank: the importance of brine release to the under ice boundary layer, *The Cryosphere*, in preparation, 2012. 130

Hunke, E. C., Notz, D., Turner, A. K., and Vancoppenolle, M.: The multiphase physics of sea ice: a review for model developers, *The Cryosphere*, 5, 989–1009, doi:10.5194/tc-5-989-2011, 2011. 137

Lebedev, V. V.: The dependence between growth of ice in Arctic rivers and seas and negative air temperature (in Russian: rost l'da v arkticheskikh rekakh i moriakh v zavisimosti ot otritsatel'nykh temperatur vozdukha), *Problemy arktiki*, 5, 9–25, 1938.

Martin, S. and Kaufmann, P.: A field and laboratory study of wave damping by grease ice, *J. Glaciol.*, 27, 283–313, 1981. 127, 137, 142, 145

Maykut, G. A.: Large-scale heat exchange and ice production in the Central Arctic, *J. Geophys. Res.*, 87, 7971–7984, 1982. 143, 145

Maykut, G. A.: The surface heat and mass balance, in: *The Geophysics of Sea Ice*, edited by: Untersteiner, N., Plenum Press, New York, 395–463, 1986. 144

Naumann, A. K.: *Physikalische Prozesse der Meereisbildung in offenem Wasser*, Master's thesis, University of Hamburg, 2011 (in German). 128, 129, 130, 144

Newyear, K. and Martin, S.: A comparison of theory and laboratory measurements of wave propagation and attenuation in grease ice, *J. Geophys. Res.*, 102, 25091–25099, 1997. 127

Notz, D.: *Thermodynamic and Fluid-Dynamical Processes in Sea Ice*, PH.D. thesis, University of Cambridge, UK, 2005. 131

## Initial sea-ice growth in open water

A. K. Naumann et al.

Title Page

Abstract

Introduction

Conclusions

References

Tables

Figures

◀

▶

◀

▶

Back

Close

Full Screen / Esc

Printer-friendly Version

Interactive Discussion



- Notz, D. and Worster, M. G.: In situ measurements of the evolution of young sea ice, *J. Geophys. Res.*, 113, C03001, doi:10.1029/2007JC004333, 2008. 139
- Notz, D. and Worster, M. G.: Desalination processes of Sea Ice, *J. Geophys. Res.*, 114, C05006, doi:10.1029/2008JC004885, 2009. 139
- 5 Omstedt, A.: Modelling frazil ice and grease ice formation in the upper layer of the ocean, *Cold Reg. Sci. Technol.*, 11, 87–98, 1985. 137
- Shen, H. H., Ackley, S. F., and Yuan, Y.: Limiting diameter of pancake ice, *J. Geophys. Res.*, 109, C12035, doi:10.1029/2003JC0021232004, 2004. 127
- 10 Smedsrud, L. H.: Frazil-ice entrainment of sediment: large-tank laboratory experiments, *J. Glaciol.*, 47, 461–471, 2001. 130, 131
- Smedsrud, L. H. and Skogseth, R.: Field measurements of Arctic grease ice properties and processes, *Cold Reg. Sci. Technol.*, 44, 171–183, 2006. 141
- Stefan, J.: Über die Theorie der Eisbildung, insbesondere über die Eisbildung im Polarmeere, *Sb. Kais. Akad. Wiss., Wien, Math.-Naturwiss.*, 98, 965–983, 1889 (in German). 127, 143, 144
- 15 Weast, R. C.: *Handbook of Chemistry and Physics*, 52 edn., Chemical Rubber Co., Cleveland, OH, 1971. 135
- Weeks, W. F. and Ackley, S. F.: The growth, structure, and properties of sea ice, in: *Geophysics of Sea Ice*, edited by: Untersteiner, N., Plenum Press, New York, 9–164, 1986. 137
- 20 Wells, A. J., Wettlaufer, J. S., and Orszag, S. A.: Brine fluxes from growing sea ice, *Geophys. Res. Lett.*, 38, L04501, doi:10.1029/2010GL046288, 2011. 139
- Wettlaufer, J. S., Worster, M. G., and Huppert, H. E.: Natural convection during solidification of an alloy from above with application to the evolution of sea ice, *J. Fluid Mech.*, 344, 291–316, 1997. 139, 140
- 25 Wilkinson, J. P., DeCarolis, G., Ehlert, I., Notz, D., Evers, K.-U., Jochmann, P., Gerland, S., Nicolaus, M., Hughes, N., Kern, S., de la Rosa, S., Smedsrud, L., Sakai, S., Shen, H., and Wadhams, P.: Ice tank experiments highlight changes in sea ice types, *EOS T. Am. Geophys. Un.*, 90, 81–82, 2009. 127
- Worster, M. G.: Instabilities of the liquid and mushy regions during solidification of alloys, *J. Fluid Mech.*, 237, 649–669, 1992. 139
- 30

## Initial sea-ice growth in open water

A. K. Naumann et al.

Title Page

Abstract

Introduction

Conclusions

References

Tables

Figures

◀

▶

◀

▶

Back

Close

Full Screen / Esc

Printer-friendly Version

Interactive Discussion



**Table 1.** CTD sensor depths during the different general setups.

CTD	quiescent	with waves	with current
top	8 cm	8 cm	8 cm
middle	32 cm	38 cm	44 cm
bottom	62 cm	74 cm	71 cm
floor	85 cm	85 cm	85 cm

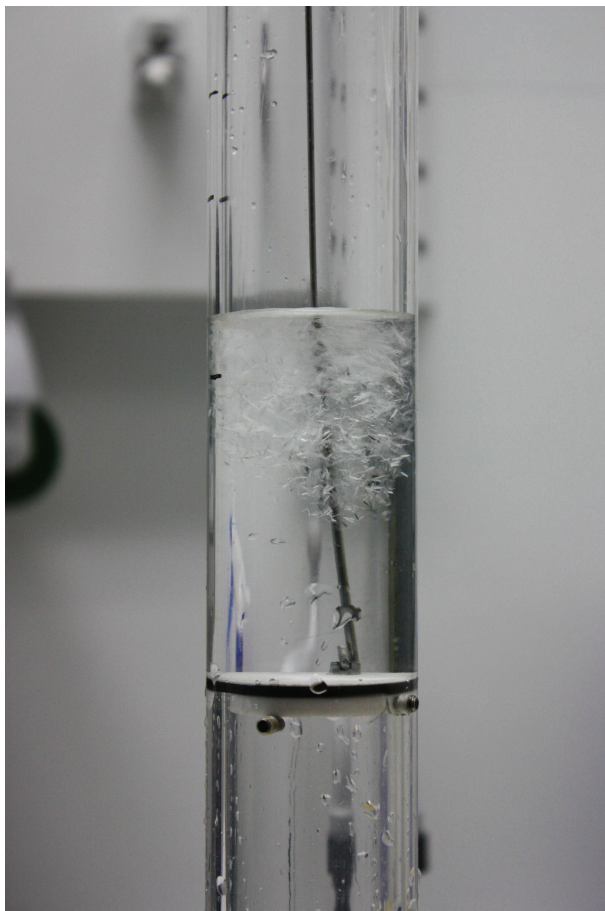
## Initial sea-ice growth in open water

A. K. Naumann et al.

**Table 2.** Resulting error of the calculated solid fraction due to measurement inaccuracy for the three methods. For all methods one has additionally a measurement inaccuracy of the grease-ice layer thickness of  $\Delta h_i = 0.5$  cm and the sample height  $\Delta h_s = 0.5$  cm. The resulting error of the solid fraction is calculated with the Gauß's error propagation law (applied to Eqs. 2, 3 and 4).

salinity	volume	calorimeter
$\Delta S_t = 0.3 \text{ g kg}^{-1}$	$\Delta V_1 = 0.25 \text{ ml}$	$\Delta I = 0.01 \text{ A}$
$\Delta S_w = 0.3 \text{ g kg}^{-1}$	$\Delta V_2 = 0.25 \text{ ml}$	$\Delta U = 0.1 \text{ V}$
	$\Delta \rho_i = 1.5 \text{ kg m}^{-3}$	$\Delta(\Delta t) = 0.5 \text{ s}$
	$\Delta \rho_{w,1} = 1.5 \text{ kg m}^{-3}$	$\Delta(\Delta T) = 1.0 \text{ }^\circ\text{C}$
	$\Delta \rho_{w,2} = 1.5 \text{ kg m}^{-3}$	$\Delta m_t = 1.0 \text{ g}$
$\Delta \phi = 0.03$	$\Delta \phi = 0.24$	$\Delta \phi = 0.02$

[Title Page](#)
[Abstract](#)
[Introduction](#)
[Conclusions](#)
[References](#)
[Tables](#)
[Figures](#)
[I◀](#)
[▶I](#)
[◀](#)
[▶](#)
[Back](#)
[Close](#)
[Full Screen / Esc](#)
[Printer-friendly Version](#)
[Interactive Discussion](#)

**Fig. 1.** Photo of the sampling device with the circular plate in horizontal position keeping the sampled grease ice trapped in the pipe.

## Initial sea-ice growth in open water

A. K. Naumann et al.

Title Page

Abstract

Introduction

Conclusions

References

Tables

Figures

◀

▶

◀

▶

Back

Close

Full Screen / Esc

Printer-friendly Version

Interactive Discussion



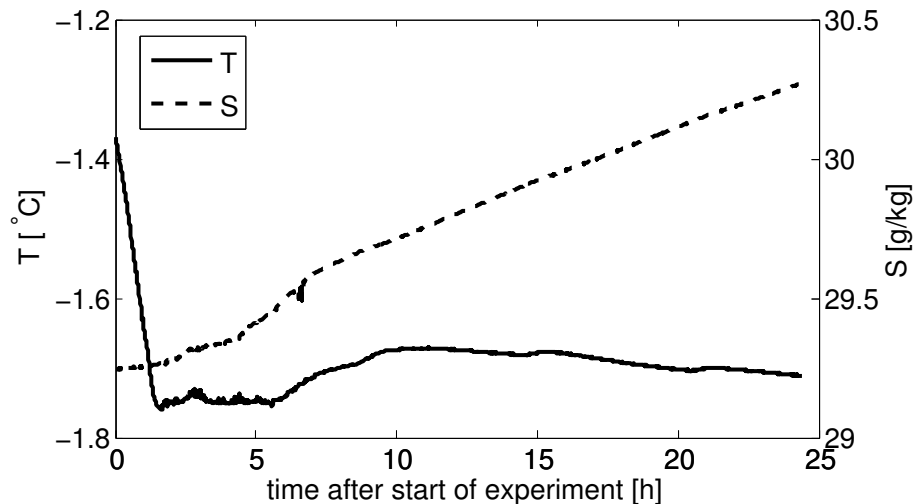


**Fig. 2.** Development of water temperature and salinity in the tank in one of the experiment with a current (air temperature at  $-15^{\circ}\text{C}$ ). Temperatures and salinities are vertical averages over the four CTDs measuring at different depths in the tank (see Table 1).

**Initial sea-ice growth in open water**

A. K. Naumann et al.

Title Page

Abstract Introduction

Conclusions References

Tables Figures

◀ ▶

◀ ▶

Back Close

Full Screen / Esc

Printer-friendly Version

Interactive Discussion



## Initial sea-ice growth in open water

A. K. Naumann et al.

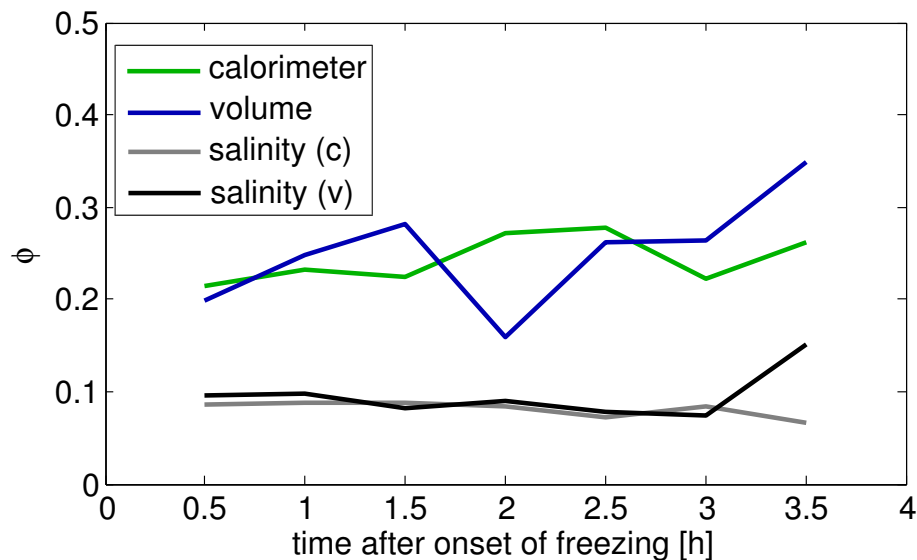


**Fig. 3.** Temporal evolution of the solid fraction as an average over all experiments with waves and with a current analysed with different methods. At each time of measurement two samples were taken, the first one analysed with the calorimeter and the salinity (c) method, the second one analysed with the volume and the salinity (v) method.

Title Page

Abstract

Introduction

Conclusions

References

Tables

Figures

◀

▶

◀

▶

Back

Close

Full Screen / Esc

Printer-friendly Version

Interactive Discussion



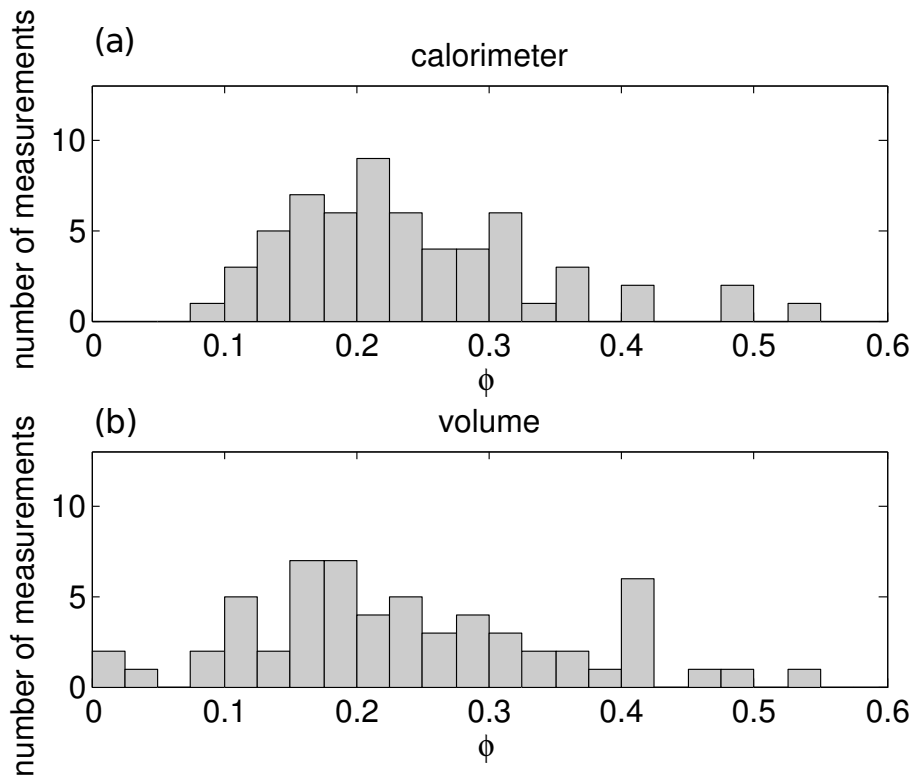


**Fig. 4.** Histogram of the solid fraction of un-consolidated grease ice for all experiments with waves and with a current determined with **(a)** the calorimeter method and **(b)** the volume method.

**Initial sea-ice growth in open water**

A. K. Naumann et al.

Title Page

Abstract Introduction

Conclusions References

Tables Figures

◀ ▶

◀ ▶

Back Close

Full Screen / Esc

Printer-friendly Version

Interactive Discussion



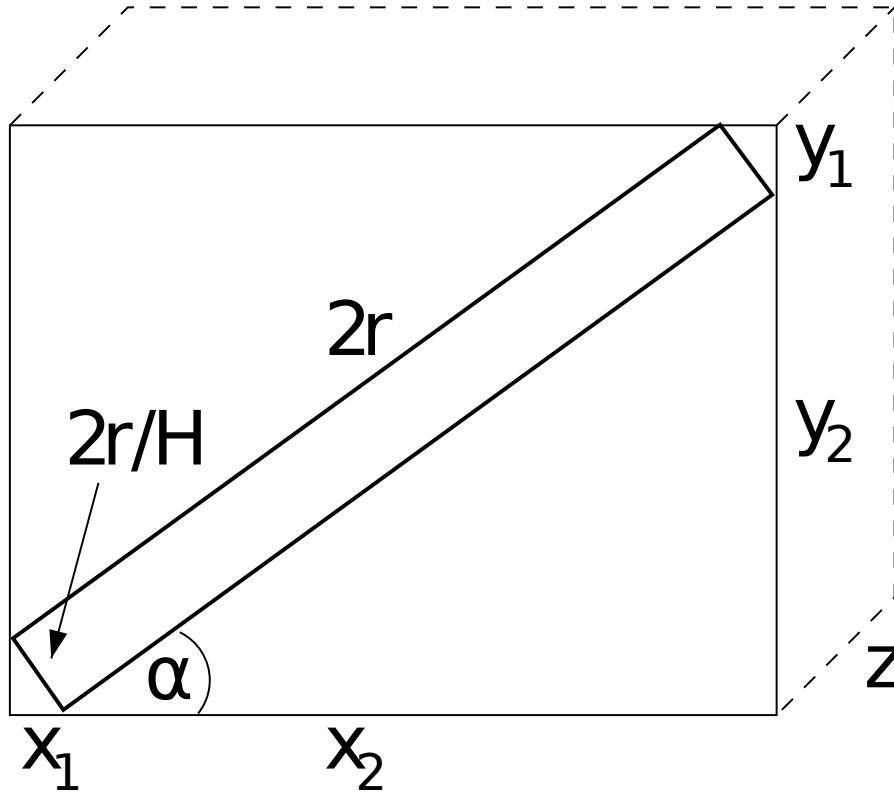


**Fig. 5.** Sketch of a disc in a cuboid:  $x_1 = \frac{2r}{H} \sin \alpha$ ,  $x_2 = 2r \cos \alpha$ ,  $y_1 = \frac{2r}{H} \cos \alpha$ ,  $y_2 = 2r \sin \alpha$  and  $z = 2r$ .

**Initial sea-ice growth  
in open water**

A. K. Naumann et al.

Title Page	
Abstract	Introduction
Conclusions	References
Tables	Figures
◀	▶
◀	▶
Back	Close
Full Screen / Esc	
Printer-friendly Version	
Interactive Discussion	



## Initial sea-ice growth in open water

A. K. Naumann et al.

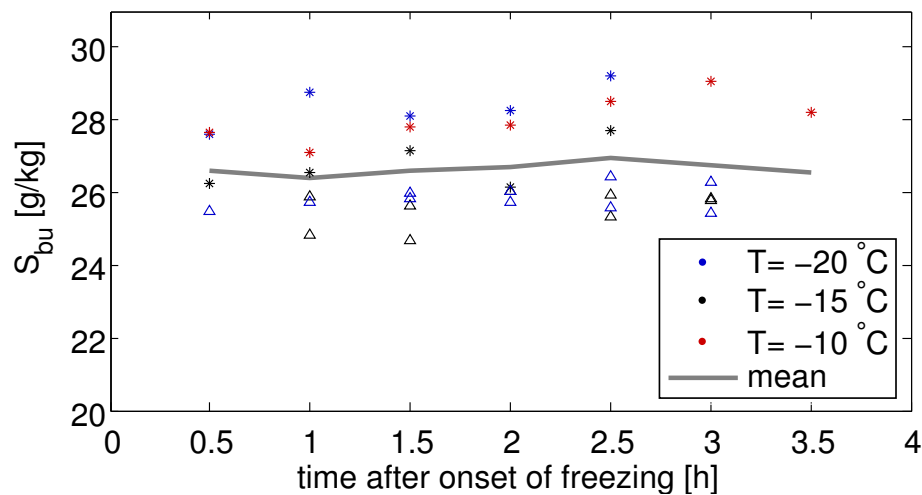


**Fig. 6.** Temporal evolution of the bulk salinity in the experiments with waves (triangle) and with a current (stars) at different air temperatures.

Title Page

Abstract

Introduction

Conclusions

References

Tables

Figures

◀

▶

◀

▶

Back

Close

Full Screen / Esc

Printer-friendly Version

Interactive Discussion



Initial sea-ice growth  
in open water

A. K. Naumann et al.

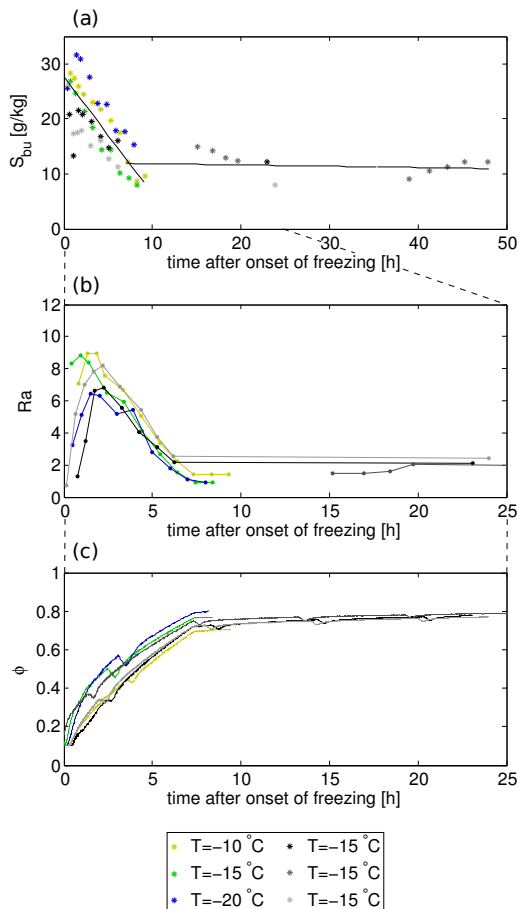


**Fig. 7.** Temporal evolution of **(a)** the bulk salinity, **(b)** the Rayleigh number and **(c)** the solid fraction in the different quiescent experiments. Color coding of the experiments corresponds to the legend at the bottom.

Title Page

Abstract

Introduction

Conclusions

References

Tables

Figures

◀

▶

◀

▶

Back

Close

Full Screen / Esc

Printer-friendly Version

Interactive Discussion



Initial sea-ice growth  
in open water

A. K. Naumann et al.

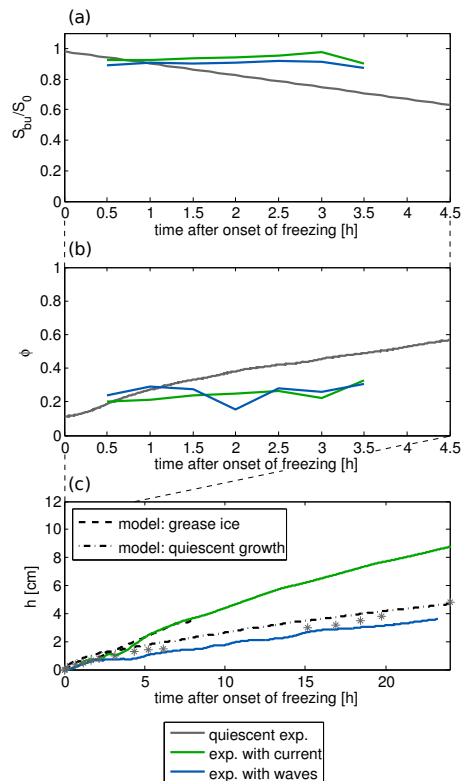


**Fig. 8.** (a) Temporal evolution of the bulk salinity normalised with the initial salinity of the water as an average over all experiments of each setup. (b) Temporal evolution of the solid fraction as an average over all experiments of each setup. In case of the experiments with waves and with a current the values shown are averages of the two reliable methods (calorimeter and volume). (c) Temporal evolution of the measured and modeled ice thickness for experiments with different general setup at an air temperature of  $-15^{\circ}\text{C}$ . Color coding of the experiments corresponds to the legend at the bottom.

Title Page

Abstract

Introduction

Conclusions

References

Tables

Figures

◀

▶

◀

▶

Back

Close

Full Screen / Esc

Printer-friendly Version

Interactive Discussion

